Reports

Microwave Spectrometer on the Nimbus 5 Satellite: Meteorological and Geophysical Data

Abstract. *The Nimbus 5 microwave spectrometer has been used to measure thermal radiation in five frequency bands between 22.235 and 58.8 gigahertz, and has yielded both the temperature profile and, over ocean, the vapor and liquid water content of the terrestrial atmosphere, even in overcast conditions. Information has also been obtained on geophysical parameters that affect the surface emissivity, such as ice type, sea roughness, and snow cover. The experiment demonstrates the considerable potential of passive microwave sensing of meteorological and geophysical parameters.*

We report here preliminary results form the Nimbus 5 (Nimbus E) microwave spectrometer (NEMS), which is making the first passive microwave measurements of global atmospheric temperature profiles as well as measurements of atmospheric water content and other geophysical parameters. One purpose of the experiment is to evaluate these techniques for operational meteorological use.

Earlier passive microwave instruments on spacecraft have measured the temperature of Venus (*1*) and the atmospheric water content and surface parameters of the earth (*2*). A similar experiment has been performed with the NEMS instrument on an aircraft (*3*), and the general techniques have been reviewed elsewhere (*4*).

The Nimbus 5 experimental earth-observatory satellite was launched on 11 December 1972 into a nearly circular sun-synchronous orbit at an inclination of 80° and an altitude of 592 nautical miles (1 nautical mile = 1852 m). Equator crossings occur near noon and midnight.

The five-channel NEMS was fabricated at the California Institute of Technology Jet Propulsion Laboratory. It views nadir with half-power beam widths of 10°. Individual channels are located on a weak water vapor resonance, in a spectral window, and at three positions on the edge of the oxygen absorption band (5-mm wavelength); the respective center frequencies are 22.235, 31.4, 53.65, 54.9, and 58.8 Ghz.

Each channel is an independent superheterodyne, load-switched radiometer with pass bands from 10 to 110 Mhz on each side of its center frequency. After synchronous detection, the data from each channel are integrated and then dumped at 2-second intervals into a ten-bit analog-digital converter. These digital words are then interleaved with an equal amount of instrument housekeeping data and stored prior to transmission to ground stations.

The instrument is calibrated every 256 seconds by means of two blackbody sources at temperatures near 215 K and 296 K. These calibration source temperatures are monitored by thermistors with a sensitivity of 0.05 K. The relative calibration of the instrument from one day to the next is believed to be better than 0.2 K, and the absolute accuracy is believed to be approximately 2 K. On the ground the data are averaged over time intervals of 16 seconds, which yields a root-mean-square sensitivity of 0.1 to 0.2 K.

The output of the NEMS is calibrated, as is customary for microwave radiometers, in terms of antenna temperature T_A, which is proportional to the power received by the antenna and is equal to the temperature of an equivalently radiating blackbody. Approximately 95 percent of the T_A is contributed by that portion of the earth within view of the main beam of the antenna; small corrections are made for the other 5 percent.

The major preliminary results of the experiment are suggested in Fig. 1, which presents the T_A values observed for orbits 163 and 210 in December 1972. The channels are numbered in order of increasing frequency. Considerable structure is evident in channels 1 and 2. These two channels clearly mark the sea-land boundaries and the regions of high humidity over ocean. The sea-land boundary is prominent because land has an emissivity of 0.7 to 1.0, whereas ocean has an emissivity near 0.5 and yields a T_A near 150 K. Since atmospheric water is much warmer than the background signal of 150 K, the water vapor resonance appears in emission over ocean. The resonance is obscured over land because of the warmer background signal. Liquid water in clouds and rain exhibits nonresonant absorption approximately proportional to the square of the frequency and also appears in emission over ocean. Over ocean these two phases of water can be estimated separately because water vapor produces a response two to three times greater in channel 1, which is on the water vapor resonance, than that in channel 2, whereas liquid water produces a response two times greater in channel 2 than in channel 1 (*3*, *5*).

In orbit 163 the intertropical convergence zone (ITCZ) is evident near the equator. In that orbit the liquid water content of the atmosphere, which is approximately proportional to the deviation of channel 2 from the nominal polar ocean values, is a maximum in two ITCZ rain bands at the edges of a humid region. In orbit 210 there are two heavy cloud regions at mid-latitudes. The small deflections of channels 1 and 2 which occur in orbit 163 near 40°N are apparently caused by ocean foam and waves. Such sea-state effects seldom increase the liquid water

Scoreboard for Reports: In the past few weeks the editors have received an average of 68 Reports per week and have accepted 12 (17 percent). We plan to accept about 12 reports per week for the next several weeks. In the selection of papers to be published we must deal with several factors: the number of good papers submitted, the number of accepted papers that have not yet been published, the balance of subjects, and length of individual papers.

Authors of Reports published in *Science* find that their results receive good attention from an interdisciplinary audience. Most contributors send us excellent papers that meet high scientific standards. We seek to publish papers on a wide range of subjects, but financial limitations restrict the number of Reports published to about 15 per week. Certain fields are overrepresented. In order to achieve better balance of content, the acceptance rate of items dealing with physical science will be greater than average.

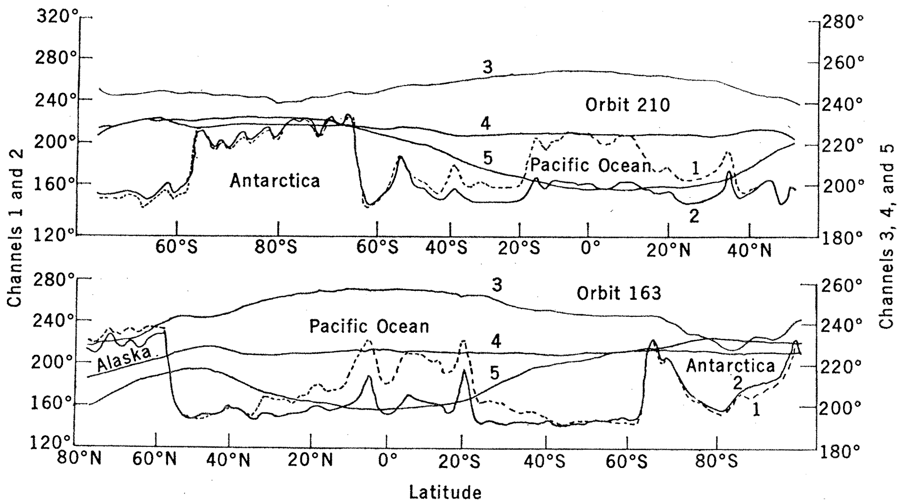

Fig. 1. Antenna temperatures (in kelvins) observed by the NEMS during portions of orbits 163 and 210 on 23 and 26 December 1972, respectively.

value by more than 0.03 g/cm^2, whereas liquid water estimates range from 0 to 0.2 g/cm^2.

In both of these orbits the atmospheric water vapor content, which is approximately proportional to the separation between channels 1 and 2, has a maximum value near the equator and exhibits features such as the sharp gradient in orbit 163 near 35°N. The inferred abundances of water vapor typically range from 0 to 5 g/cm^2, and preliminary comparisons with nearby radiosonde data yield errors typically less than 0.4 g/cm^2.

Emissions from various types of snow and ice are also evident in Fig. 1. Because the atmospheric transmissivity below 35 Ghz is typically greater than 80 percent and because the atmospheric temperature is approximately equal to the surface brightness temperature, it follows that atmospheric effects are not generally apparent over land or ice. Alaska is characterized by T_A values that are lower in channel 2 than in channel 1. This spread diminishes at the north coast of Alaska, where there is a band of newer ice. The spread then increases farther north where the ice is older. The ice spectrum may result from scattering from ice inhomogeneities. As the ice ages, scattering could be enhanced as the salt content slowly concentrates and drains away, thus increasing the number of voids and the ice transmissivity. The very low T_A values, below 220 K, also imply that ice scattering is important. Similar effects have been noted by Wilheit *et al.* (*6*) during observations from aircraft.

In central Antarctica T_A in channels 1 and 2 is even lower, and approaches 160 K in orbit 163. Orbit 210 skirted this central region, and the T_A is thus higher. Although scattering from inhomogeneities in the ice and snow presumably occurs here too, the spectral dependence is the reverse of that noted for sea ice. Central Greenland exhibits similar behavior.

Channels 3, 4, and 5 respond primarily to the atmospheric temperature profile. The microwave emission spectrum is related to the temperature profile because each emission frequency originates from a specific atmospheric layer approximately 10 km thick, as was first noted by Meeks and Lilley (*7*). Near the center of the 5-mm oxygen absorption band the atmosphere is extremely opaque and the received radiation originates from high altitudes, whereas in the wings of the complex the radiation originates low in the atmosphere. The radiation measured in channels 3, 4, and 5 of the NEMS originates in layers centered near 4, 11, and 18 km, respectively.

The general features of the global pattern of atmospheric temperatures are evident in Fig. 1. The channel 3 T_A values, corresponding to the lower troposphere, are cooler toward the poles, whereas the stratospheric channel 5 is cooler near the equator, except for the cold region evident near Alaska.

One important unexpected result of the experiment is the observed lack of significant discontinuities in T_A *for* channels 3 through 5 attributable to atmospheric temperature or to clouds. Over the latitude range from 10°N to 15°S the peak-to-peak variation for channel 3 is typically 1 to 2 K, and the largest variations are associated with the ITCZ. In the ITCZ high dense clouds decrease the brightness temperature by 0 to 4 K, in most cases by 0 to 1.5 K. These ITCZ-induced variations generally extend over 3° to 5° of latitude and are sometimes spatially unresolved. Two such variations are barely observable in orbit 163 over each of the ITCZ bands evident in channels 1 and 2. Excluding the ITCZ, the peak-to-peak variations in the channel 3 T_A values over this region are generally less than 1 K; this result implies that temperature gradients can be determined with considerable accuracy. This demonstration of the relative insensitivity of the instrument to clouds is one of the principal results of the NEMS experiment.

Another source of channel 3 varia-

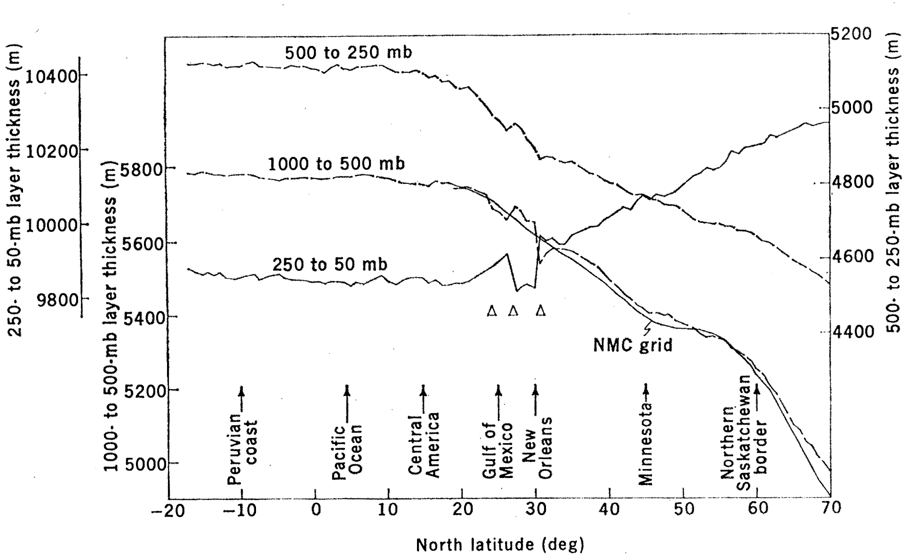

Fig. 2. Layer thicknesses determined from NEMS data during orbit 1133 on 5 March 1973 (day 64). The NMC grid data are from NMC 0^h and 12^h analyses interpolated in time and space so as to correspond to the subsatellite point.

tions is land of high elevation, such as exists in Antarctica, Greenland, and the Himalayas, where the landmass occupies the same altitude region as the channel 3 weighting function. Such variations, which can reach 10 to 20 K, are evident over Antarctica in Fig. 1. Only a few high mountainous regions cause variations greater than 2 K, and the effect either can be compensated for or can be ignored in these restricted areas. Channels 4 and 5 respond exclusively to the atmospheric temperature profile and are unaffected by clouds or the terrestrial surface.

The microwave data are compared with conventional meteorological data in Fig. 2, which presents preliminary estimates of thicknesses for three atmospheric layers for 5 March 1973. The 1000- to 500-mb layer is the layer of air ranging from a pressure of 1000 mb to a pressure of 500 mb. Its thickness is proportional to its average temperature; an increase of 1 K corresponds to an increase of ~20 m. The pressures 1000, 500, 250, and 50 mb roughly correspond to altitudes of 0, 5, 10, and 20 km, respectively. Temperature changes of 1 K correspond to layer thickness changes of ~20 and ~47 m for the 500- to 250-mb and 250- to 50-mb layers, respectively.

We estimated the layer thicknesses by computing for each layer an appropriate linear function of T_A for channels 3, 4, and 5, where the coefficients minimize the root-mean-square error expected for that season and region (*3*). For this purpose the globe was divided into three ocean and four land regions, the boundaries of which are indicated in Fig. 2 by small triangles. The small discontinuities in inferred layer thickness at these boundaries are thus artifacts. The depression of 80 m (~4 K) in the NEMS-inferred 1000- to 500-mb thickness which occurs near New Orleans results from a major storm with high dense clouds. Such variation is rare outside the ITCZ.

Also shown in Fig. 2 is the 1000- to 500-mb layer thickness derived from the National Meteorological Center (NMC) analyses. For most of the orbit the difference between the NMC and NEMS data is approximately 20 m or 1 K. This agreement between NMC and NEMS data suggests that microwave measurements could be a very useful source of meteorological data.

Inaccuracies in the layer thickness estimates above 500 mb are, at this time, caused principally by errors in instrument calibration and in the expressions for atmospheric transmission. Preliminary analysis of these errors suggests that increasing the pressure dependence of the 58.8-Ghz absorption coefficient significantly improves the layer thickness estimates.

Preliminary estimates of temperature profile accuracy have also been evaluated. Temperature profiles are estimated by computing, for each altitude of interest, an appropriate linear function of T_A for channels 3, 4, and 5, using the statistical procedure described earlier and an a priori global ensemble of atmospheres. Temperature profiles determined from the NEMS differ from those interpolated from selected regions of the NMC 0^h and 12^h Northern Hemisphere analyses by 1.5 to 4 K (root mean square) over the altitude range from 1 to 20 km. The largest discrepancies occur near the tropopause and at the surface where large temperature gradients are more common. These preliminary results appear to be consistent with the 0.8- to 3-K (root mean square) errors predicted for a noiseless ıadiometer and perfect NMC analyses.

The NEMS experiment has thus demonstrated the ability of microwave spectrometers to yield estimates of atmospheric temperature profiles in the presence of most cloud types and, over ocean, the abundances of atmospheric water vapor and liquid water. Additional information about ice and snow cover, soil moisture, and sea state is also contained in the data. It is expected that future microwave temperature-sounding systems with more frequency channels and spatial scanning will be capable of complete global coverage over the altitude range from 0 to 80 km.

D. H. STAELIN, A. H. BARRETT
J. W. WATERS
Research Laboratory of Electronics, Massachusetts Institute of Technology, Cambridge 02139
F. T. BARATH, E. J. JOHNSTON
P. W. ROSENKRANZ
Jet Propulsion Laboratory, California Institute of Technology, Pasadena
N. E. GAUT
Environmental Research and Technology, Inc., Lexington, Massachusetts 02173
W. B. LENOIR
Johnson Spacecraft Center, National Aeronautics and Space Administration, Houston, Texas 77058

References and Notes

1. F. T. Barath, A. H. Barrett, J. Copeland, D. E. Jones, A. E. Lilley, *Astron. J.* **69**, 49 (1964).
2. A. E. Basharinov, A. S. Gurvich, S. T. Yegorov, *Dokl. Akad. Nauk SSSR* **188**, 1273 (1969).
3. P. W. Rosenkranz, F. T. Barath, J. C. Blinn III, E. J. Johnston, W. B. Lenoir, D. H. Staelin, J. W. Waters, *J. Geophys. Res.* **77**, 5833 (1972).
4. D. H. Staelin, *Proc. Inst. Electr. Electron. Eng.* **57**, 427 (1969).
5. ———, *J. Geophys. Res.* **71**, 2875 (1966).
6. T. Wilheit, W. Nordberg, J. Blinn, W. Campbell, A. Edgerton, *Remote Sensing Environ.* **2**, 129 (1973).
7. M. L. Meeks and A. E. Lilley, *J. Geophys. Res.* **68**, 1683 (1963).
8. We thank W. Nordberg for critical help in the establishment of this experimental program. We also thank J. C. Blinn III for help with the instrument calibration, and K. Kunzi, R. Pettyjohn, and R. K. L. Poon for developing many of the data-reduction computer programs. This work was suported by NASA contract NAS7-100.

14 August 1973

Micrometeorite Craters Discovered on Chondrule-Like Objects from Kapoeta Meteorite

Abstract. *Craters attributable to hypervelocity impacts of micrometeorites have been discovered on rare chondrule-like objects from the gas-rich meteorite Kapoeta. These chondrule-like objects, probably generated by impacts themselves, provide further evidence for the regolith origin of Kapoeta. The micrometeorite flux at the time of formation of the meteorites was probably an order of magnitude higher than the present flux, but the solar luminosity could not have been higher than 1.7 times its present value.*

The Kapoeta meteorite is a typical gas-rich meteorite which contains high concentrations of helium, neon, and argon. The rare gas excess is generally believed to be the result of solar wind implantation because it is confined to the outer ~ 10^{-5} cm of mineral grains (*1*) and has relative abundance ratios similar to those observed in the sun. Roughly 10 percent of the grains in Kapoeta are "track-rich" grains (*2, 3*) attributable to strong irradiation by low-energy (~ 1 Mev per nucleon) iron-group nuclei from solar flares. The density and radial gradient of tracks in the track-rich grains indicate that these grains were exposed to solar flare particles for times on the order of 10^4 years (*2, 3*), with negligible shielding ($<10^{-3}$ g cm^{-2}). The nonuniformity